

## ONLINE FIRST

## Fragile X–Associated Tremor/Ataxia Syndrome

## Influence of the FMR1 Gene on Motor Fiber Tracts in Males With Normal and Premutation Alleles

Jun Yi Wang, PhD; David Hessel, PhD; Andrea Schneider, PhD; Flora Tassone, PhD; Randi J. Hagerman, MD; Susan M. Rivera, PhD

**Importance:** Individuals with the fragile X premutation express expanded CGG repeats (repeats 55-200) in the *FMR1* gene and elevated *FMR1* messenger RNA (mRNA) levels, both of which may underlie the occurrence of the late-onset neurodegenerative disorder fragile X–associated tremor/ataxia syndrome (FXTAS). Because the core feature of FXTAS is motor impairment, determining the influence of *FMR1* mRNA levels on structural connectivity of motor fiber tracts is critical for a better understanding of the pathologic features of FXTAS.

**Objective:** To examine the associations of CGG repeat and *FMR1* mRNA with motor-related fiber tracts in males with premutation alleles.

**Design and Setting:** A case-control study conducted at the University of California, Davis, from April 1, 2008, through August 31, 2009. All data were collected masked to the carrier status of the *FMR1* gene.

**Participants:** Thirty-six male premutation carriers with FXTAS and 26 male premutation carriers without FXTAS were recruited through their family relationships with children affected by fragile X syndrome. The controls were 34 unaffected family members and healthy volunteers from the local community.

**Main Outcomes and Measures:** The CGG repeat lengths and *FMR1* mRNA expression levels in peripheral blood lymphocytes, motor functioning, and white matter structural integrity that were estimated using dif-

fusion tensor imaging. After data collection, we selected 4 motor tracts to reconstruct using diffusion tensor tractography, namely, the middle and superior cerebellar peduncles, descending motor tracts (containing the corticospinal, corticobulbar, and corticopontine tracts), and the anterior body of the corpus callosum.

**Results:** All fiber tracts exhibited weaker structural connectivity in the FXTAS group (decreased 5%-53% from controls,  $P \leq .02$ ). Genetic imaging correlation analysis revealed negative associations of CGG repeat length and *FMR1* mRNA with connectivity strength of the superior cerebellar peduncles in both premutation groups (partial  $r^2=0.23-0.33$ ,  $P \leq .004$ ). In addition, the measurements from the corpus callosum and superior cerebellar peduncles revealed a high correlation with motor functioning in all 3 groups ( $r$  between partial least square predicted and actual test scores = 0.41-0.56,  $P \leq .04$ ).

**Conclusions and Relevance:** Distinct pathophysiologic processes may underlie the structural impairment of the motor tracts in FXTAS. Although both the corpus callosum and superior cerebellar peduncles were of great importance to motor functioning, only the superior cerebellar peduncles exhibited an association with the elevated RNA levels in the blood of fragile X premutation carriers.

*JAMA Neurol.* Published online June 10, 2013.  
doi:10.1001/jamaneurol.2013.2934

**T**HE FRAGILE X MENTAL RETARDATION 1 (*FMR1*) gene contains a polymorphic trinucleotide CGG repeat in its 5' untranslated region. The repeat sizes normally range from 5 to 44 but exceed 200 in full mutation, which effectively silences the gene, causing intellectual disability in fragile X syndrome.<sup>1,2</sup> CGG repeats from 55 to 200 are within the premutation range. Although the *FMR1* protein levels are only slightly reduced in the premutation alleles, the *FMR1* messenger

RNA (mRNA) levels are significantly elevated<sup>3,4</sup> and thought to cause the neurodegenerative disorder fragile X–associated tremor/ataxia syndrome (FXTAS).<sup>5,6</sup> FXTAS is a late-onset neurodegenerative disorder that affects approximately 40% of males with premutation alleles and who are older than 50 years.<sup>7</sup> A constellation of clinical features is linked to FXTAS, with progressive intention tremor and cerebellar ataxia presenting as core features.<sup>8</sup>

Structural magnetic resonance imaging (MRI) has the advantage of revealing dis-

Author Affiliations are listed at the end of this article.

**Table 1. Characteristics of the 96 Research Participants**

Characteristic	Healthy Controls		Fragile X–Associated Tremor/Ataxia Syndrome (FXTAS)			
	No. of Participants	Mean (SD) [Range]	Negative		Positive	
			No. of Participants	Mean (SD) [Range]	No. of Participants	Mean (SD) [Range]
Age, y	34	43.6 (18.4) [18-81]	26	44.4 (16.4) [20-76]	36	65.7 (7.2) [50-79] <sup>a,b</sup>
Age for older participants, y	15	62.3 (8.1) [51-81]	9	62.8 (9.6) [50-76]	36	65.7 (7.2) [50-79]
CGG length	34	28.2 (4.47) [19-42]	26	88.9 (25.3) [55-157] <sup>a</sup>	36	96.5 (20.9) [62-154] <sup>a</sup>
<i>FMR1</i> mRNA level	34	1.49 (0.25) [1.0-2.0]	24	2.84 (1.08) [1.4-6.4] <sup>a</sup>	36	3.11 (0.84) [1.6-5.6] <sup>a</sup>
Behavioral tests						
BDS-2	32	22.4 (3.01) [17-27]	25	22.1 (2.80) [15-26]	35	15.8 (5.67) [4-25] <sup>a,b</sup>
Purdue Pegboard Dexterity Test <sup>c</sup>	29	39.7 (6.50) [26-57]	25	38.1 (5.13) [28-48]	32	23.5 (6.96) [8-35] <sup>a,b</sup>

Abbreviations: BDS-2, Behavioral Dyscontrol Scale 2; mRNA, messenger RNA.

<sup>a</sup>Significantly different from the control group ( $P \leq .05$ ).

<sup>b</sup>Significantly different from the FXTAS-negative group ( $P \leq .05$ ).

<sup>c</sup>Total test scores for both hands were used.

ease progress in vivo. Previous studies revealed T2 hyperintensities in the middle cerebellar peduncle (MCP), widespread gray matter atrophy and white matter structural impairment, and, a negative correlation between CGG repeat length and brain volume, MCP packing density, and gray matter density of the dorsomedial frontal lobes.<sup>9-14</sup> Given that motor deficits are the core clinical features and the prominent involvement of the cerebellum in the pathophysiologic function of FXTAS, it is critical to examine the RNA toxic effect (ie, RNA toxic gain-of-function due to excess *FMR1* mRNA)<sup>3,4,15</sup> on motor fiber tracts for a better understanding of the pathologic features of FXTAS. In the current study, we reconstructed motor-related fiber tracts from diffusion tensor imaging (DTI)<sup>16</sup> and tested the associations of CGG repeat length and *FMR1* mRNA with structural connectivity of these motor tracts in premutation carriers with and without FXTAS.

## METHODS

### RESEARCH PARTICIPANTS

We recruited 62 male premutation carriers through their family relationships with children affected by fragile X syndrome from April 1, 2008, through August 18, 2009, before a major scanner upgrade that resulted in incomparable DTIs before and after the upgrade. Unaffected family members, along with healthy males recruited from the local community, served as controls ( $n=34$ ). These controls and 26 of the premutation carriers were the same participants in a recent investigation of age-related changes in fragile X premutation.<sup>13</sup> We identified premutation alleles using *FMR1* DNA testing<sup>17</sup> and measured *FMR1* mRNA using a quantitative-fluorescence reverse transcription-polymerase chain reaction method.<sup>4</sup> In addition, we assessed FXTAS stage with tremor or ataxia intensity,<sup>8,18</sup> behavioral self-regulation using the Behavioral Dyscontrol Scale 2,<sup>19</sup> and dexterity using the Purdue Pegboard Dexterity Test.<sup>20</sup> We diagnosed 36 carriers as being affected by FXTAS, ranging from FXTAS stage 2 (minor tremor or balance problems with no interference in daily living) to 5 (use of a wheelchair on a daily basis). In multiple regression analysis with age as a covariate, we found that although the FXTAS-negative group showed simi-

lar motor abilities as the controls, the FXTAS-positive group exhibited deficits in behavioral self-regulation and dexterity (**Table 1**).

### STANDARD PROTOCOL APPROVALS, REGISTRATIONS, AND PATIENT CONSENTS

All participants signed informed consent forms issued by the institutional review boards at the University of California, Davis.

### NEUROIMAGE ACQUISITION AND PROCESSING

We performed neuroimaging from an MRI scanner with an 8-channel head coil (Siemens Trio 3T MRI scanner; Siemens Medical Solutions). We obtained DTIs with 30 gradient directions using a single-shot, diffusion-weighted echo planar imaging sequence in 72 axial sections of 1.9-mm thickness (no gap) with a 243-mm field of view and a 128 × 128 matrix. The diffusion sensitizing gradients were applied at a  $b$  of value 700 s/mm<sup>2</sup>. Five additional images with minimum diffusion weighting were also obtained.

### NEUROIMAGE PROCESSING

The DTI processing and tractography have been described in detail in a previous study.<sup>13</sup> To summarize, we used the FSL software package (<http://fsl.fmrib.ox.ac.uk/fsl/fslwiki/>; University of Oxford) for performing eddy current and motion correction and skull stripping.<sup>21</sup> We conducted DTI tractography in DTI Studio (<http://www.mristudio.org>; The Johns Hopkins Medical Institute) by applying a multiple regions-of-interest approach.<sup>22</sup> The fractional anisotropy (FA) threshold for fiber tracking was set at 0.18 and the angle threshold at 70°. The tractography methods have been previously tested,<sup>13</sup> and all measurements reached an intraclass correlation coefficient of 0.9 or more. Fiber tracking was performed masked to the status of the participants.

We reconstructed 4 motor-related fiber tracts: (1) the descending motor tract containing the corticospinal, corticopontine, and corticobulbar tracts; (2) the MCP; (3) the superior cerebellar peduncle (SCP); and (4) the anterior body of the corpus callosum (CC; containing primarily the transcallosal fibers for the premotor and supplementary motor areas). Tractography measurements were FA for assessing fiber directionality, mean dif-

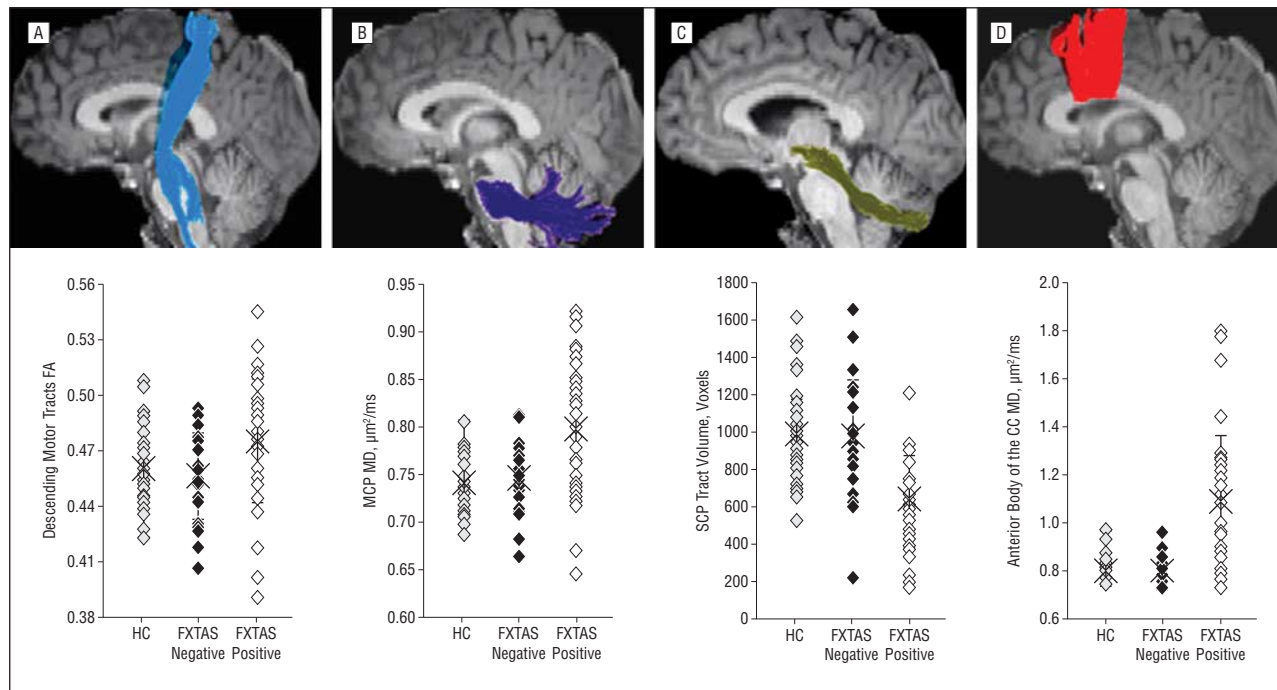


**Figure 1.** The 4 reconstructed fiber tracts and their representative measurements for the 3 groups. The original values are shown in the graphs. A, The descending motor tracts showing elevated fractional anisotropy (FA) in carriers with fragile X-associated tremor/ataxia syndrome (FXTAS) compared with the older healthy controls (HCs) ( $\beta = .024, P = .01$ ). B, The middle cerebellar peduncle (MCP) showing elevated mean diffusivity (MD) in carriers with FXTAS compared with older controls ( $\beta = .058, P = .003$ ). C, The superior cerebellar peduncle (SCP) showing reduced tract volume in carriers with FXTAS compared with the older controls ( $\beta = -248, P < .001$ ). D, The MD of the anterior body of the corpus callosum (CC) was elevated in carriers with FXTAS compared with the older controls ( $\beta = .22, P = .002$ ).

fusivity (MD) for packing density, and tract volume for the number of voxels occupied by the reconstructed fiber tract. To account for individual differences in cranial size, total cranial volume was estimated from the T1-weighted MPRAGE images using the SIENAX function<sup>23</sup> from FSL and was used to normalize tract volumes.

## STATISTICAL ANALYSIS

We divided the participants into 3 groups: FXTAS-positive, FXTAS-negative, and control groups. We were able to consider not only the effect of having FXTAS but also the potential differential effect of *FMRI* premutation alleles and normal alleles on motor fiber tracts. We applied multiple linear regression analyses to compare both premutation groups with the control group and to predict individual tractography measurements using either CGG repeat length or *FMRI* mRNA level. Because all premutation carriers with FXTAS were 50 years or older, only older healthy controls ( $\geq 50$  years) were included in the comparisons of the FXTAS group with the control group. We used age as a covariate for multiple linear regression. We constructed residual plots to identify possible violations of the assumptions in linear regression and repeated analysis using ranks<sup>24</sup> in case of violation. To predict motor functioning from the combination of 12 tractography measurements, we conducted partial least square (PLS) regression,<sup>25</sup> which decomposed the independent and dependent variables simultaneously to find a set of latent variables explaining the maximum covariance. The quality of the prediction was assessed by calculating Pearson product moment correlation coefficient and paired *t* test between the original and predicted test scores. The importance of individual tractography measurements to the predictions were assessed by the Pearson product moment correlation coefficient between the tractography measurements and PLS factors. We cross-validated the PLS results using the leave-

one-out procedure in which we took out the participants one by one and predicted their test scores using the tractography measurements from the remaining participants. A separate PLS regression was performed for each group and for each test because of missing test scores for some of the participants. To correct for multiple comparisons, we applied the Benjamini-Hochberg method of false discovery rate (FDR) to all analyses.<sup>26</sup> All statistical analyses were conducted using the Matlab software package (version 7.10.0; The Mathworks Inc).

## RESULTS

### GROUP COMPARISONS

The 4 fiber tracts (**Figure 1**) were reconstructed successfully for all participants, including the 3 carriers at FXTAS stage 5. In group comparisons, 9 tractography measurements survived the 5% FDR ( $P \leq .02$ ). When compared with the older control group, the FXTAS-positive group had significantly lower tract volume of all 4 fiber tracts; higher MD of the SCP, MCP, and CC; lower FA of the SCP; and higher FA of the descending motor tract. In contrast, none of the tractography measurements had any group differences between the FXTAS-negative and control groups even at the level of raw  $P = .05$  (Figure 1 and **Table 2**).

To determine whether the FA elevation in the FXTAS-positive group was due to the degeneration of an intersecting tract (the posterior body of the CC), we performed an analysis similar to the one performed in our previous publication.<sup>13</sup> This study revealed that degeneration of the body and splenium of the CC led to arti-

**Table 2. Group Mean (SD) and Comparisons of Tractography Measurements**

Variable	HCs (n = 34)	FXTAS Negative (n = 26)	$\beta$ (95% CI) for FXTAS Negative vs HCs (df = 2,57)	P Value <sup>a</sup>	Older HCs (n = 15)	FXTAS Positive (n = 36)	$\beta$ (95% CI) for FXTAS Positive vs Older HCs (df = 2,48)	P Value <sup>a</sup>
Descending motor tracts								
Tract volume, voxels	1287 (354)	1264 (276)	-23.2 (-193 to 147)	.79	1265 (327)	942 (360)	-321 (-545 to -97)	<b>.006</b>
Fractional anisotropy	0.46 (0.02)	0.46 (0.02)	-0.003 (-0.014 to 0.008)	.59	0.45 (0.02)	0.48 (0.03)	0.024 (0.005 to 0.043)	<b>.01</b>
Mean diffusivity, $\mu\text{m}^2/\text{ms}$	0.82 (0.03)	0.82 (0.04)	-0.005 (-0.021 to 0.010)	.50	0.84 (0.03)	0.87 (0.07)	0.023 (-0.014 to 0.059)	.21
Middle cerebellar peduncle								
Tract volume, voxels	2931 (543)	2868 (517)	-58.7 (-334 to 217)	.67	2982 (521)	2553 (502)	-400 (-721 to -79)	<b>.02</b>
Fractional anisotropy	0.50 (0.02)	0.49 (0.02)	-0.003 (-0.013 to 0.008)	.60	0.50 (0.02)	0.48 (0.04)	-0.016 (-0.039 to 0.007)	.16
Mean diffusivity, $\mu\text{m}^2/\text{ms}$	0.74 (0.03)	0.75 (0.03)	0.007 (-0.009 to 0.023)	.40	0.74 (0.03)	0.80 (0.07)	0.058 (0.020 to 0.096)	<b>.003</b>
Super cerebellar peduncle								
Tract volume, voxels	761 (189)	757 (225)	-5.34 (-111 to 101)	.92	815 (152)	556 (210)	-248 (-372 to -124)	<b>&lt;.001</b>
Fractional anisotropy	0.47 (0.03)	0.47 (0.03)	-0.010 (-0.022 to 0.002)	.09	0.50 (0.02)	0.48 (0.03)	-0.024 (-0.042 to -0.006)	<b>.008</b>
Mean diffusivity, $\mu\text{m}^2/\text{ms}$	0.98 (0.06)	0.99 (0.05)	0.013 (-0.017 to 0.044)	.39	0.96 (0.04)	1.06 (0.09)	0.087 (0.037 to 0.136)	<b>.001</b>
Corpus callosum anterior body								
Tract volume, voxels	1920 (488)	1960 (451)	49.9 (-164 to 263)	.64	1662 (499)	780 (581)	-750 (-1055 to -446)	<b>&lt;.001</b>
Fractional anisotropy	0.56 (0.03)	0.55 (0.02)	-0.004 (-0.016 to 0.008)	.51	0.54 (0.03)	0.53 (0.04)	-0.007 (-0.031 to 0.018)	.59
Mean diffusivity, $\mu\text{m}^2/\text{ms}$	0.80 (0.05)	0.80 (0.05)	-0.001 (-0.023 to 0.021)	.95	0.83 (0.06)	1.09 (0.27)	0.217 (0.085 to 0.348)	<b>.002</b>

Abbreviations: FXTAS, fragile X-associated tremor/ataxia syndrome; HCs, healthy controls.

<sup>a</sup>Bold P values are significant at a false discovery rate of 5%;  $P \leq .02$  for multiple regression using age as a covariate.

ficially increased FA of the cerebral peduncular projections to the parietal lobes. We identified axial sections 48 to 56 as the zone in which the descending motor tracts intersect with the CC and, consequently, calculated the mean FA value for these sections (eFigure; <http://www.jamaneurol.com>). The FXTAS-positive group indeed had significantly elevated FA compared with the older controls after adjusting for age. We also observed that another zone, from axial sections 42 to 48, had elevated FA in the FXTAS-positive group and identified superior fronto-occipital fasciculus<sup>27,28</sup> as the intersecting fiber tract.

#### CORRELATION WITH CGG LENGTH AND *FMRI* mRNA

Five tractography measurements survived the 5% FDR ( $P = .007$ ) and demonstrated significant associations with CGG repeat length and/or *FMRI* mRNA. The CGG repeat length correlated negatively with the SCP tract volume in the FXTAS-positive and FXTAS-negative groups and with SCP FA in the FXTAS-positive group only. In addition, *FMRI* mRNA had a negative correlation with SCP FA in the FXTAS-positive group (Figure 2) and CC FA in the control group (partial  $r^2 = 0.31$ ,  $P < .001$ ).

Three premutation carriers had extremely high *FMRI* mRNA levels ( $\geq 3$  SDs). We thus repeated multiple linear regression using rank-ordered data. The results were comparable. The only differences were that SCP MD instead of SCP FA significantly correlated with *FMRI* mRNA in the FXTAS-positive group, and the correlation between SCP track volume and *FMRI* mRNA became significant at an FDR of 5% ( $P = .007$ ) using rank-ordered data.

#### CORRELATION WITH MOTOR FUNCTIONING

The PLS regression could predict all motor test scores from the tractography measurements for the 3 groups. Therefore, only the results from the leave-one-out cross-validation have been chosen for presentation. Three tests survived the 5% FDR ( $P \leq .02$ ), indicating the significant correlation between the actual and predicted motor test scores (Table 3). The tractography measurements predicted behavioral regulation and dexterity for the FXTAS-positive carriers and behavioral regulation for the controls. The tractography measurements predicted behavioral regulation of FXTAS-negative carriers to a lesser degree, with this value passing the 10% FDR

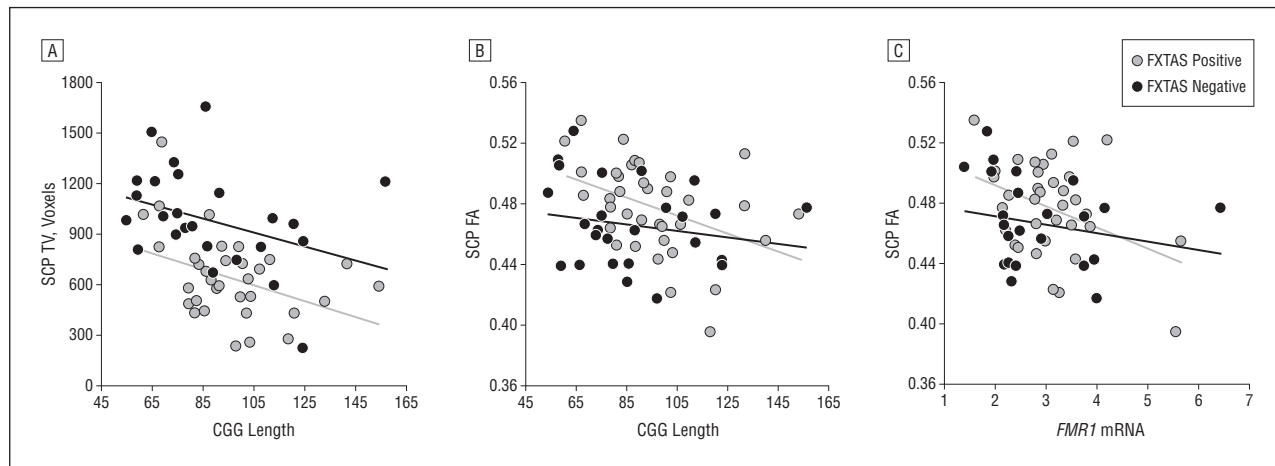


**Figure 2.** Tractography measurements showing associations with the *FMR1* gene. The original values are displayed in the graphs. A, The tract volume (TV) of the superior cerebellar peduncle (SCP) showed negative correlation with CGG length in both the fragile X-associated tremor/ataxia syndrome (FXTAS) negative (partial  $r_{3,22}^2 = 0.33$ ,  $P = .004$ ) and FXTAS-positive (partial  $r_{3,32}^2 = 0.24$ ,  $P = .003$ ) groups. B, The SCP fractional anisotropy (FA) showed a negative correlation with CGG repeat length in the FXTAS-positive group (partial  $r_{2,33}^2 = 0.29$ ,  $P = .001$ ). C, The SCP also showed a negative correlation between FA and *FMR1* messenger RNA in the FXTAS-positive group (partial  $r_{2,33}^2 = 0.23$ ,  $P = .003$ ).

**Table 3. Partial Least Square Regression Using Motor Tract Measurements (X) to Predict Motor Test Scores (Y)<sup>a</sup>**

Behavioral Tests, Groups	Behavioral Dyscontrol Scale 2			Purdue Pegboard Dexterity Test		
	Healthy Controls	Fragile X-Associated Tremor/Ataxia Syndrome		Healthy Controls	Fragile X-Associated Tremor/Ataxia Syndrome	
		Negative	Positive		Negative	Positive
No. of participants	32	25	35	29	25	32
Explained variance of X, %	28.9	14.5	28.4	24.7	17.3	24.8
Explained variance of Y, %	37.0	42.3	47.0	34.9	36.6	51.5
Correlation (Y, predicted Y)						
<i>R</i>	0.41	0.42	0.55	0.31	0.02	0.56
<i>P</i> value	<b>.02</b>	.037 <sup>b</sup>	<b>&lt;.001</b>	.10	.91	<b>&lt;.001</b>
Paired <i>t</i> test (Y, predicted Y)						
<i>df</i>	31	24	34	28	24	31
<i>T</i>	-0.005	0.120	-0.094	0.006	0.176	-0.059
95% CI	-1.0 to 1.0	-1.2 to 1.3	-1.8 to 1.6	-2.4 to 2.4	-2.5 to 3.0	-2.1 to 2.0
<i>P</i> value	>.99	.90	.93	>.99	.86	.95

<sup>a</sup>The results from the jackknife are shown. Bold *P* values are significant at a false discovery rate of 5% for Pearson correlation between Y and predicted Y ( $P \leq .02$ ).

<sup>b</sup>Significant at a false discovery rate of 10% ( $P \leq .04$ ).

( $P = .04$ ). Consistent with the PLS results, none of the paired *t* tests showed significant differences between the actual and predicted motor scores (Table 3). In the PLS regression, measurements from the CC and SCP made substantial contributions to the predictions of motor tests for all the 3 groups, whereas those from the descending motor tracts and MCP were important to the predictions of dexterity in both premutation groups.

We further analyzed the correlation using penalized regression with the Least Absolute Shrinkage and Selection Operator,<sup>29</sup> which predicted the 2 motor tests for the FXTAS-positive group. However, it did not predict any test scores for the other 2 groups (eAppendix).

## DISCUSSION

This study investigated the link among the *FMR1* gene, motor-related fiber tracts, and motor functioning in males

with premutation and normal alleles. Two motor fiber tracts, the SCP and the anterior body of the CC, had significant associations with the *FMR1* gene and motor functioning. Specifically, we found that both increased CGG repeat length and *FMR1* mRNA correlated with lower SCP connectivity in the FXTAS-positive and FXTAS-negative groups. We also found that *FMR1* mRNA elevation correlated with reduced CC connectivity in the control group. In addition, measurements from the CC and SCP exhibited high correlation with motor functioning in all 3 groups.

Carrying most of the efferent fibers from the cerebellum,<sup>30</sup> the SCP has a critical role in motor functioning and may be a key structure manifesting the RNA toxicity associated with fragile X premutation. The current study demonstrated a negative dose effect of CGG repeat length and *FMR1* mRNA on the connectivity strength of SCP in premutation carriers both with and without

FXTAS. Our results are consistent with pathophysiologic findings of FXTAS, including marked dropout of Purkinje cells, white matter disease throughout the cerebellum, and the presence of intranuclear inclusions in the inferior olivary and dentate nuclei.<sup>31,32</sup> Most of the SCP fibers originate in the deep nuclei (dentate and interposed nuclei), which receive the projections from the Purkinje cells, the only cell type carrying the output from the cerebellar cortex.<sup>30</sup> It is reasonable to assume that the negative association between the SCP and the expanded CGG repeats is related to the degeneration of both dentate nucleus and Purkinje cells. Further studies are needed to investigate the particular vulnerability of SCP to the CGG expansion and *FMRI* mRNA elevation.

Additional major findings are related to the CC. Previous studies of FXTAS have reported thinning,<sup>14</sup> FA reduction,<sup>12</sup> and high variability of the tractography measurements of the CC, which correlated with carriers' FXTAS stage.<sup>13</sup> The current results extend these findings by revealing a significantly reduced structural connectivity of this fiber tract in the FXTAS-positive group and the relationship between *FMRI* mRNA and CC FA in the control group. However, in the premutation carriers, the correlation between *FMRI* mRNA and the CC was not significant; in contrast, the CC displayed progressive degeneration with increasing FXTAS stage.<sup>13</sup> It is conceivable that the combination of *FMRI* mRNA levels remaining stable throughout adulthood<sup>33</sup> and the CC connectivity worsening with FXTAS severity contributed to the disappearance of this correlation in the premutation groups.

In addition, the changes in the CC measurements with FXTAS progression might not be linear, potentially making the situation even more complex. The anterior body of the CC had higher FA and lower MD in some of the patients at the early stages of FXTAS compared with the controls, whereas the directions of change reversed at the advanced stage. The early changes in FA and MD were unlikely caused by the crossing-fiber issue in DTI. Although the degeneration of one crossing fiber tract would lead to artificial elevation of FA for the surviving fiber tract, MD would also increase because of the less restricted water diffusion. The pattern of DTI changes at early stages of FXTAS could be explained by axonal swelling because of mitochondrial dysfunction that has been detected in premutation carriers regardless of FXTAS status.<sup>34</sup> One consequence of mitochondrial dysfunction is impaired axonal transport, which relies on mitochondria for its energy supply.<sup>33,35</sup> This process leads to accumulation of cellular organelles within the axons, consistent with the early DTI representations. At advanced stages of FXTAS, however, we observed decreased FA and increased MD compared with healthy controls in some of the patients, which was consistent with axonal degeneration. Support for these assumptions comes from mitochondrial DNA mutations in which MD reduction in acute lesions and MD elevation in chronic lesions have been reported.<sup>36</sup> This complex pattern of DTI changes could also explain why the correlation with *FMRI* mRNA was not observed in the FXTAS-negative group. The FXTAS-negative group was composed of premutation carriers with heterogeneous phenotypes. Some members may

develop FXTAS later in their lives, whereas others may not. To confirm, longitudinal studies combining neuroimaging and molecular data will be valuable for delineating the dynamic changes of DTI measurements as FXTAS progresses and pathophysiologic mechanisms underlying the DTI changes.

Regarding the MCP, we failed to replicate the quadratic relationship between CGG length and the MCP diffusivity observed when premutation carriers with and without FXTAS were combined in another study.<sup>12</sup> The MCP carries efferent fibers from the pontine nucleus to almost all areas of the cerebellar cortex<sup>30</sup> and is the structure that has shown T2 hyperintensive signals (the MCP sign) in a subset of FXTAS carriers<sup>14</sup>; therefore, the MCP is used as one of the criteria for diagnosing FXTAS.<sup>8</sup> In the current cohort, the MCP sign was detected in all 26 carriers at stages 3 to 5, 3 of 10 carriers at stage 2, and 1 of 11 carriers at stage 0, whereas none of the controls showed the MCP sign. Consistent with these neurologic observations, significantly elevated MCP MD was detected in the carriers with FXTAS compared with the controls. However, the MCP sign may actually involve both the MCP and SCP. The SCP is a relatively small structure and shares pathways with the MCP in the cerebellar white matter core. Although visual inspection of T2 signal intensity is useful for clinical diagnosis, the SCP cannot be distinguished well in a clinical read. Tractography in DTI has the advantage of obtaining less subjective, quantitative measurements for correlational analyses, as well as having the capability to distinguish the SCP from the MCP. In the current study, the CGG repeat length had a robust correlation with the reconstructed SCP but not with the MCP even when the FXTAS-positive and FXTAS-negative groups were combined. Differences in methods may account for these discrepancies. The previous DTI study<sup>12</sup> conducted tract-of-interest and voxel-based analyses that required image normalization to a standard space to define the anatomical location of a fiber tract. The current study performed DTI tractography in participants' native spaces to localize a fiber tract. In the brains with severe atrophy, the SCP may be best quantified using tractography in participants' native space to minimize distortion during image normalization.

Another intriguing finding is the relative sparing of the descending motor tracts in contrast to the severe degeneration of the corpus callosum body despite the fact that the fibers from these 2 structures may terminate in the same cortical areas. Further studies are needed to identify neuroprotective factors that prevent descending motor tracts from the RNA toxicity in fragile X premutation.<sup>15</sup>

The current study is limited by the well-known crossing-fiber issue in the fiber tracking algorithm, which may cause early termination of fiber propagation or absent fiber branches. Small sample sizes, especially in the case of the FXTAS-negative premutation group ( $n = 26$ ), may provide insufficient powers to detect a real effect. The *FMRI* mRNA levels, which have shown high variability among different tissues, were obtained from peripheral blood leukocytes and thus may not completely reflect the correspondent values in the CNS.<sup>37</sup> Because many analyses were performed, there is a need to replicate the study in other samples, which, if consistent or largely consis-

tent with the current findings, would make false discovery of an effect much less likely. The association of reduced FMR1 protein seen in some premutation carriers<sup>4,38,39</sup> with structural connectivity is an important remaining question that we hope to explore in future studies. Finally, we conducted a separate study<sup>40</sup> to further examine the correlation between FMR1 mRNA and brain measurements (including the anterior body of the CC) in the control group.

In conclusion, we demonstrate the relevance of the motor fiber tracts to FXTAS, finding associations with both RNA toxicity and motor impairment. Because FXTAS is an age-related neurodegenerative disorder that commonly affects male fragile X premutation carriers older than 50 years, clinicians and researchers should target male premutation carriers 40 years or older for early diagnosis, disease monitoring, and potential treatment. Alternations in the motor fiber tracts detected by imaging techniques may prove to be effective biomarkers of early development of FXTAS in future studies.

**Accepted for Publication:** March 11, 2013.

**Published Online:** June 10, 2013. doi:10.1001/jamaneurol.2013.2934

**Author Affiliations:** Center for Mind and Brain (Drs Wang and Rivera) and Department of Psychology (Dr Rivera), University of California, Davis; and Departments of Psychiatry and Behavioral Sciences (Drs Wang and Hessler), Pediatrics (Drs Schneider and Hagerman), and Biochemistry and Molecular Medicine (Dr Tassone) and Medical Investigation of Neurodevelopmental Disorders (MIND) Institute (Drs Hessler, Schneider, Tassone, Hagerman, and Rivera), University of California, Davis, Medical Center, Sacramento.

**Correspondence:** Susan M. Rivera, PhD, Center for Mind and Brain, 202 Cousteau Pl, Ste 250, Davis, CA 95618 (srivera@ucdavis.edu).

**Author Contributions:** *Study concept and design:* Wang, Hessler, Hagerman, and Rivera. *Acquisition of data:* Wang, Hessler, Schneider, and Tassone. *Analysis and interpretation of data:* Wang, Schneider, and Rivera. *Drafting of the manuscript:* Wang. *Critical revision of the manuscript for important intellectual content:* All authors. *Statistical analysis:* Wang. *Obtained funding:* Hessler, Hagerman, and Rivera. *Administrative, technical, and material support:* Schneider and Hagerman. *Study supervision:* Hessler, Hagerman, and Rivera. *Consult for assessments:* Schneider.

**Conflict of Interest Disclosures:** Dr Wang receives support as a postdoctoral fellow from grant TL1DA024854 from the National Institutes of Health. Dr Hessler receives support from Roche, Novartis, and Seaside Therapeutics for treatment trials in fragile X syndrome and research support from grants MH078041 and MH077554 from the National Institutes of Health. Dr Tassone receives research support from grant HD02274 from the National Institutes of Health. Dr Hagerman receives grant support from Roche, Novartis, Seaside Therapeutics, Forest, and Curemark for treatment trials in fragile X or autism and research support from grants RL1AG032115, UL1DE0199583, and HD036071 from the National Institutes of Health, and the National Fragile X Foundation. Dr Rivera receives research support from grants

MH078041 and NS062412 from the National Institutes of Health.

**Funding/Support:** This work was supported by grants HD036071 (Dr Hagerman), HD02274 (Dr Tassone), MH078041 (Dr Hessler), MH077554 (Drs Hessler and Rivera), NS062412 (Dr Rivera), UL1DE019583 (Dr Hagerman), RL1AG032115 (Dr Hagerman), and TL1DA024854 (Dr Wang) from the National Institutes of Health.

**Online-Only Material:** The eFigure and eAppendix are available at <http://www.jamaneurol.com>.

**Additional Contributions:** John Wang, BA, and Patrick Adams, BA, performed image and data collection. Tom Porteous, PhD, provided editorial comments. Danielle Harvey, PhD, provided statistical support. We thank the research participants and their families.

## REFERENCES

1. Verkerk AJ, Pieretti M, Sutcliffe JS, et al. Identification of a gene (FMR-1) containing a CGG repeat coincident with a breakpoint cluster region exhibiting length variation in fragile X syndrome. *Cell*. 1991;65(5):905-914.
2. Devys D, Lutz Y, Rouyer N, Bellocq JP, Mandel JL. The FMR-1 protein is cytoplasmic, most abundant in neurons and appears normal in carriers of a fragile X premutation. *Nat Genet*. 1993;4(4):335-340.
3. Tassone F, De Rubeis S, Carosi C, et al. Differential usage of transcriptional start sites and polyadenylation sites in FMR1 premutation alleles. *Nucleic Acids Res*. 2011;39(14):6172-6185.
4. Tassone F, Hagerman RJ, Taylor AK, Gane LW, Godfrey TE, Hagerman PJ. Elevated levels of FMR1 mRNA in carrier males: a new mechanism of involvement in the fragile-X syndrome. *Am J Hum Genet*. 2000;66(1):6-15.
5. Hoem G, Raske CR, Garcia-Arocena D, et al. CGG-repeat length threshold for FMR1 RNA pathogenesis in a cellular model for FXTAS. *Hum Mol Genet*. 2011;20(11):2161-2170.
6. Hagerman RJ, Leehey M, Heinrichs W, et al. Intention tremor, parkinsonism, and generalized brain atrophy in male carriers of fragile X. *Neurology*. 2001;57(1):127-130.
7. Jacquemont S, Hagerman RJ, Leehey MA, et al. Penetrance of the fragile X-associated tremor/ataxia syndrome in a premutation carrier population. *JAMA*. 2004;291(4):460-469.
8. Berry-Kravis E, Abrams L, Coffey SM, et al. Fragile X-associated tremor/ataxia syndrome: clinical features, genetics, and testing guidelines. *Mov Disord*. 2007;22(14):2018-2030.
9. Loesch DZ, Litewka L, Brotchie P, Huggins RM, Tassone F, Cook M. Magnetic resonance imaging study in older fragile X premutation male carriers. *Ann Neurol*. 2005;58(2):326-330.
10. Cohen S, Masyn K, Adams J, et al. Molecular and imaging correlates of the fragile X-associated tremor/ataxia syndrome. *Neurology*. 2006;67(8):1426-1431.
11. Hashimoto R, Javan AK, Tassone F, Hagerman RJ, Rivera SM. A voxel-based morphometry study of grey matter loss in fragile X-associated tremor/ataxia syndrome. *Brain*. 2011;134(pt 3):863-878.
12. Hashimoto R, Srivastava S, Tassone F, Hagerman RJ, Rivera SM. Diffusion tensor imaging in male premutation carriers of the fragile X mental retardation gene. *Mov Disord*. 2011;26(7):1329-1336.
13. Wang JY, Hessler DH, Hagerman RJ, Tassone F, Rivera SM. Age-dependent structural connectivity effects in fragile X premutation. *Arch Neurol*. 2012;69(4):482-489.
14. Brunberg JA, Jacquemont S, Hagerman RJ, et al. Fragile X premutation carriers: characteristic MR imaging findings of adult male patients with progressive cerebellar and cognitive dysfunction. *AJNR Am J Neuroradiol*. 2002;23(10):1757-1766.
15. Hagerman PJ. Current gaps in understanding the molecular basis of FXTAS [published online May 18, 2012]. *Tremor Other Hyperkinet Mov (N Y)*. 2012;2:tre-02-63-375-2.
16. Basser PJ, Pierpaoli C. Microstructural and physiological features of tissues elucidated by quantitative-diffusion-tensor MRI. *J Magn Reson B*. 1996;111(3):209-219.
17. Tassone F, Pan R, Amiri K, Taylor AK, Hagerman PJ. A rapid polymerase chain reaction-based screening method for identification of all expanded alleles of the fragile X (FMR1) gene in newborn and high-risk populations. *J Mol Diagn*. 2008;10(1):43-49.
18. Bacalman S, Farzin F, Bourgeois JA, et al. Psychiatric phenotype of the fragile

- X-associated tremor/ataxia syndrome (FXTAS) in males: newly described fronto-subcortical dementia. *J Clin Psychiatry*. 2006;67(1):87-94.
19. Grigsby J, Kaye K, Robbins LJ. Reliabilities, norms and factor structure of the Behavioral Dyscontrol Scale. *Percept Mot Skills*. 1992;74(3 pt 1):883-892.
  20. Tiffin J, Asher EJ. The Purdue pegboard; norms and studies of reliability and validity. *J Appl Psychol*. 1948;32(3):234-247.
  21. Smith SM. Fast robust automated brain extraction. *Hum Brain Mapp*. 2002;17(3):143-155.
  22. Huang H, Zhang J, van Zijl PC, Mori S. Analysis of noise effects on DTI-based tractography using the brute-force and multi-ROI approach. *Magn Reson Med*. 2004;52(3):559-565.
  23. Smith SM, Zhang Y, Jenkinson M, et al. Accurate, robust, and automated longitudinal and cross-sectional brain change analysis. *Neuroimage*. 2002;17(1):479-489.
  24. Conover WJ, Iman RL. Rank transformations as a bridge between parametric and nonparametric statistics. *Am Stat*. 1981;35:124-129.
  25. Abdi H. Partial least squares regression and projection on latent structure regression (PLS-Regression). *Wiley Interdisciplinary Rev Computational Stat*. 2010; 2:97-106.
  26. Benjamini Y, Hochberg Y. Controlling the false discovery rate: a practical and powerful approach to multiple testing. *J R Stat Soc, B*. 1995;57:289-300.
  27. Wakana S, Jiang H, Nagae-Poetscher LM, van Zijl PC, Mori S. Fiber tract-based atlas of human white matter anatomy. *Radiology*. 2004;230(1):77-87.
  28. Schmahmann JD, Pandya DN. The complex history of the fronto-occipital fasciculus. *J Hist Neurosci*. 2007;16(4):362-377.
  29. Friedman J, Hastie T, Tibshirani R. Regularization paths for generalized linear models via coordinate descent. *J Stat Softw*. 2010;33(1):1-22.
  30. Nolte J. *The Human Brain: An Introduction to Its Functional Anatomy*. 5th ed. St Louis, MO: Mosby; 2002.
  31. Greco CM, Berman RF, Martin RM, et al. Neuropathology of fragile X-associated tremor/ataxia syndrome (FXTAS). *Brain*. 2006;129(pt 1):243-255.
  32. Greco CM, Hagerman RJ, Tassone F, et al. Neuronal intranuclear inclusions in a new cerebellar tremor/ataxia syndrome among fragile X carriers. *Brain*. 2002; 125(pt 8):1760-1771.
  33. Yrigollen CM, Tassone F, Durbin-Johnson B, Tassone F. The role of AGG interruptions in the transcription of *FMR1* premutation alleles. *PLoS One*. 2011; 6(7):e21728.
  34. Ross-Inta C, Omanska-Klusek A, Wong S, et al. Evidence of mitochondrial dysfunction in fragile X-associated tremor/ataxia syndrome. *Biochem J*. 2010; 429(3):545-552.
  35. Wang JY, Bakhadirov K, Abdi H, et al. Longitudinal changes of structural connectivity in traumatic axonal injury. *Neurology*. 2011;77(9):818-826.
  36. Friedman SD, Shaw DW, Ishak G, Gropman AL, Saneto RP. The use of neuroimaging in the diagnosis of mitochondrial disease. *Dev Disabil Res Rev*. 2010; 16(2):129-135.
  37. Tassone F, Hagerman RJ, Garcia-Arocena D, Khandjian EW, Greco CM, Hagerman PJ. Intranuclear inclusions in neural cells with premutation alleles in fragile X associated tremor/ataxia syndrome. *J Med Genet*. 2004;41(4):e43.
  38. Kenneson A, Zhang F, Hagedorn CH, Warren ST. Reduced FMRP and increased *FMR1* transcription is proportionally associated with CGG repeat number in intermediate-length and premutation carriers. *Hum Mol Genet*. 2001;10(14): 1449-1454.
  39. Hessler D, Wang JM, Schneider A, et al. Decreased fragile X mental retardation protein expression underlies amygdala dysfunction in carriers of the fragile X premutation. *Biol Psychiatry*. 2011;70(9):859-865.
  40. Wang JY, Hessler D, Iwahashi C, et al. Influence of the fragile X mental retardation (*FMR1*) gene on the brain and working memory in men with normal *FMR1* alleles. *Neuroimage*. 2013;65:288-298.